Cooperative Nucleophilic and General-Acid Catalysis by the $HisH^+$−His Pair and Arginine Transition State Binding in Catalysis of Ester Hydrolysis Reactions by Designed Helix−Loop−Helix Motifs

Kerstin S. Broo, Helena Nilsson, Jonas Nilsson, Anna Flodberg, and Lars Baltzer*

Contribution from the Department of Chemistry, Göteborg University, 412 96 Göteborg, Sweden

Received October 31, 1997

Abstract: A histidine-based two-residue reactive site for the catalysis of hydrolysis and transesterification reactions of *p*-nitrophenyl esters has been engineered into a helix in a designed helix−loop−helix motif, and it has been shown to function through cooperative nucleophilic and general-acid catalysis. The two-residue site has been expanded by the incorporation of two arginine residues in the neighboring helix, and the arginines have been found to provide further transition state binding of the anionic transition state. The second-order rate constant in aqueous solution at pH 5.1 and 290 K for the peptide with the most efficient two-residue site is 0.054 M^{-1} s^{-1}, the pK_a value of both the histidine residues, His-30 and His-34, is 5.6, and the kinetic solvent isotope effect is 1.5. The introduction of Arg-11 and Arg-15 increases the second-order rate constant to 0.105 M^{-1} s^{-1}. The second-order rate constant of a peptide with a two-residue site of His-26 and His-30 is 0.010 M^{-1} s^{-1}, and the pK_a values of the two His residues are 6.8 and 5.6, respectively. The difference in reactivity between the two peptides is consistent with a model where the His with the higher number in the sequence is the nucleophile and the His with the lower number is a general-acid catalyst. The results are incompatible with a model where the histidine residue with the lower number is the nucleophile.

Introduction

The engineering of novel catalysts that rival the efficiency and selectivity of native enzymes represents a formidable challenge due to the difficulties in organizing residues in three dimensions, and in controlling the reaction pathways. Recent advances in *de novo* protein design[1−3] now make it possible to begin to address these complex issues in model proteins. The decarboxylation of oxaloacetate[4] was accomplished by two 14-residue peptides, and the ligation of amphiphilic peptides[5] was catalyzed by a 33-residue helical sequence. The rate enhancements in both cases were on the order of 3 orders of magnitude over the rates of the uncatalyzed reactions. We have designed a polypeptide with 42 amino acid residues, KO-42, that folds into a helix−loop−helix motif and dimerizes to form a four-helix bundle.[6] On the surface of the folded polypeptide histidine residues have been introduced that catalyze hydrolysis and transesterification reactions of *p*-nitrophenyl esters with second-order rate constants that are 1140 and 620 times larger, respectively, than those of the 4-methylimidazole-catalyzed reaction at pH 4.1 and 290 K.[6] One key issue in *de novo* catalyst design is the identification and understanding of the function of sites where the interplay between two or more amino acid residues provides cooperative catalysis since competent reactive sites can be supplemented with binding residues to induce substrate specificity and serve as building blocks for sites that can catalyze a variety of reactions. We now report that the reactivity of KO-42, which has six His residues, is due to the cooperative behavior of $HisH^+$−His pairs in helical segments, where the unprotonated His residues function as nucleophiles and the protonated $HisH^+$ forms strong hydrogen bonds to one or both of the ester oxygens in the transition state. These two-residue sites represent a novel concept in polypeptide catalysis, and the $HisH^+$−His pair may be used for the engineering of a large variety of catalysts with tailor-made specificities through the introduction of flanking residues capable of transition state binding and substrate recognition.

Results and Discussion

Design and Solution Structures of the Polypeptide Catalysts. The design of the four-helix bundle motif was based on the designs and solution structures of SA-42 and KO-42 that have been described in detail previously.[6,7] The amino acid sequence of KO-42 contains 42 residues (Figure 1) and folds into a hairpin helix−loop−helix motif due to hydrophobic interactions between amphiphilic helices and dimerizes to form a four-helix bundle. The amino acid residues of KO-42 and of SA-42 were chosen on the basis of their propensity for secondary structure formation, and several features designed to stabilize the folded structure were incorporated, e.g., capping residues, residues that stabilize the helical dipole and that

(1) Raleigh, D. P.; Betz, S. F.; DeGrado, W. F. *J. Am. Chem. Soc.* **1995**, *117*, 7558−7559.
(2) Struthers, M. D.; Cheng, R. P.; Imperiali, B. *Science* **1996**, *271*, 342−345.
(3) Brive, L.; Dolphin, G. T.; Baltzer, L. *J. Am. Chem. Soc.* **1997**, *119*, 8598−8607.
(4) Johnsson, K.; Allemann, R. K.; Widmer, H.; Benner, S. A. *Nature* **1993**, *365*, 530−532.
(5) Severin, K.; Lee, D. H.; Kennan, A. J.; Ghadiri, R. M. *Nature* **1997**, *389*, 706−709.
(6) Broo, K. S.; Brive, L.; Ahlberg, P.; Baltzer, L. *J. Am. Chem. Soc.* **1997**, *119*, 11362−11372.
(7) Olofsson, S.; Johansson, G.; Baltzer, L. *J. Chem. Soc., Perkin Trans. 2* **1995**, 2047−2056.

S0002-7863(97)03758-X CCC: $15.00
Published on Web 04/18/1998

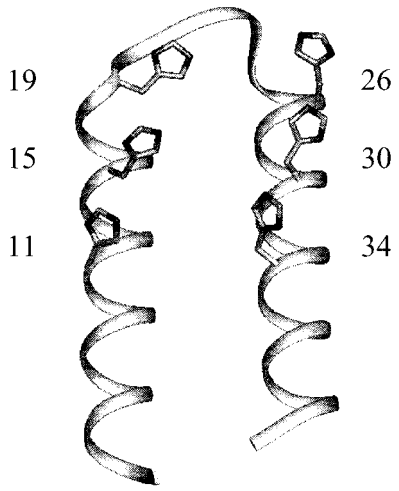

1
Ac-N-A-A-D-Nle-E-A-A-I-K-H-L-A-E-H-Nle-A-A-H

20 23
-G-P-V-D-

42
-A-A-H-Nle-A-E-H-L-A-K-H-F-E-A-F-A-R-A-G-NH_2

peptide	11	15	19	26	30	34	k_2 ($M^{-1}s^{-1}$)
MN	**H**(6.6)	**H**(5.7)	**H**(6.8)	Q	Q	A	0.027
JN	A	Q	K	**H**(6.8)	**H**(5.7)	**H**(5.7)	0.065
MNI	**H**(6.5)	**H**(6.1)	Q	Q	Q	A	0.011
MNII	A	**H**(6.0)	**H**(7.0)	Q	Q	A	0.008
JNI	A	Q	K	**H**(6.9)	**H**(5.6)	A	0.010
JNII	A	Q	K	Q	**H**(5.6)	**H**(5.6)	0.055
JNIII	A	Q	K	**H**(6.8)	Q	**H**(5.4)	0.007

Figure 1. Amino acid sequence of KO-42 in the one-letter code and the modeled structure of a helix−loop−helix motif showing the geometric relationship between the histidine residues. For clarity only the monomer is shown although KO-42 and SA-42 both have been shown to form dimers. The sequences of the modified peptides are the same as those of KO-42 except in the positions occupied by histidine residues in the sequence of KO-42. The modified residues for each peptide are shown, with the pK_a of the histidines in parentheses and the second-order rate constants for the hydrolysis of mono-*p*-nitrophenyl fumarate at pH 5.1 in aqueous solution at 290 K.

neutralize the charges at the helical termini. In order to identify the catalytic entities of KO-42, we have now synthesized several amino acid sequences (Figure 1) that are the same as that of KO-42 except that three or four of the histidines have been replaced by "unreactive" residues, most often those of the template polypeptide SA-42.[7]

The structures of KO-42 and of SA-42 have been determined by NMR and CD spectroscopy and by equilibrium sedimentation ultracentrifugation.[6−8] The mean residue ellipticities of the modified peptides reported here show that the structures have not been affected much by the few residue alterations since the variation in the absolute value of the mean residue ellipticity is less than ±10%; the measured values are in the range from −21 000 to −25 000 deg cm^2 dmol^{-1}. The mean residue ellipticities of the peptides have been shown to be independent of peptide concentration above 50 μM, and all kinetic measurements and pK_a determinations reported here have been carried out in the concentration independent region, where the peptide is predominantly folded and dimeric. The effect of pH on the mean residue ellipticity is negligible for MN, JNI, JNII, and JNIII with deviations from the value at pH 6 of 1000 deg cm^2 dmol^{-1} or less, whereas a minor effect on the ellipticity of JN at low pH was detected. The mean residue ellipticity of JN at pH 4 is −15 000 deg cm^2 dmol^{-1}.

The pK_a values of all His residues have been measured by ^{1}H NMR spectroscopy (Figure 1) in D_2O solution at 46 °C, under the usual assumption that the solvent isotope effects on the dissociation constants and the pH electrode potentials cancel out. It has been shown previously that the pK_a at 46 °C deviates by less than 0.1 unit from that at 17 °C[6] in 10 vol % trifluoroethanol. The relative concentrations of the ionizing species have been calculated using standard equations (Figure 2) in order to determine the pH at which the fully unprotonated, and noncooperative, species has a neglible effect on the observed reactivity. The pH dependence of the second-order rate constants of the KO-42-catalyzed reactions showed that the fully protonated catalyst has negligible reactivity.[6] It is shown in Figure 2 that, in the case of MN, which contains three His residues, the diprotonated species dominates in the range from 5 to 6, but in the case of JN, the diprotonated species is only the main component at a pH that is close to 5. Furthermore, in the polypeptide JNII, where both pK_a values are 5.6, the only pH range where the concentration of the monoprotonated species dominates over that of the unprotonated one is close to pH 5. Consequently, the pH that was chosen for the studies of the reactivity of the catalysts was pH 5.1 where, as a rule, the states of protonation that dominate are those expected to provide cooperative catalysis.

Reactivity of Histidine-Based Catalysts. The pH dependence and kinetic solvent isotope effects of the KO-42 catalyzed reactions showed that the larger than 1000-fold rate enhancements over that of 4-methylimidazole catalysis depend on the simultaneous occurrence of unprotonated and protonated His residues.[6] No saturation kinetics were observed, and the interactions responsible for the enhanced reactivity therefore take place in the transition state. The reactivity of KO-42 is due to six histidine residues on the surface of the folded motif (Figure 1), and seven peptides have now been synthesized that contain two or three histidines in the same sequential positions as those in KO-42. The three histidines of helix I of KO-42, His-11, His-15, and His-19 have been introduced in the polypeptide MN, and the sequence of JN contains the histidine residues of helix II of KO-42, His-26, His-30, and His-34. In a similar way the three possible two-residue His sites of helix II, His-26−His-30, His-30−His-34, and His-26−His-34, have been incorporated in the peptides JNI, JNII, and JNIII. The latter peptide was included as a reference since cooperative catalysis is not possible due to the large distance between the two His residues. The two pairwise His sites in helix I, His-11−His-15 and His-15−His-19, have been introduced in the peptides MNI and MNII, respectively.

The second-order rate constants for the peptide-catalyzed hydrolysis of mono-*p*-nitrophenyl fumarate have been determined in 100 mM sodium acetate buffer solution at pH 5.1 and 290 K (Figure 1) with peptide and substrate concentrations in the submillimolar range. Under these conditions differential salt effects are negligible. The kinetic measurements were determined under conditions of excess peptide over substrate to ensure that the second-order rate constants could be obtained from pseudo-first-order kinetics even if the reaction were to follow saturation kinetics. The background reaction at pH 5.1 is sufficiently slow that the peptide-catalyzed reaction is dominant even at submillimolar concentrations of catalyst. The

(8) Olofsson, S.; Baltzer, L. *Folding Des.* **1996**, *1*, 347−356.

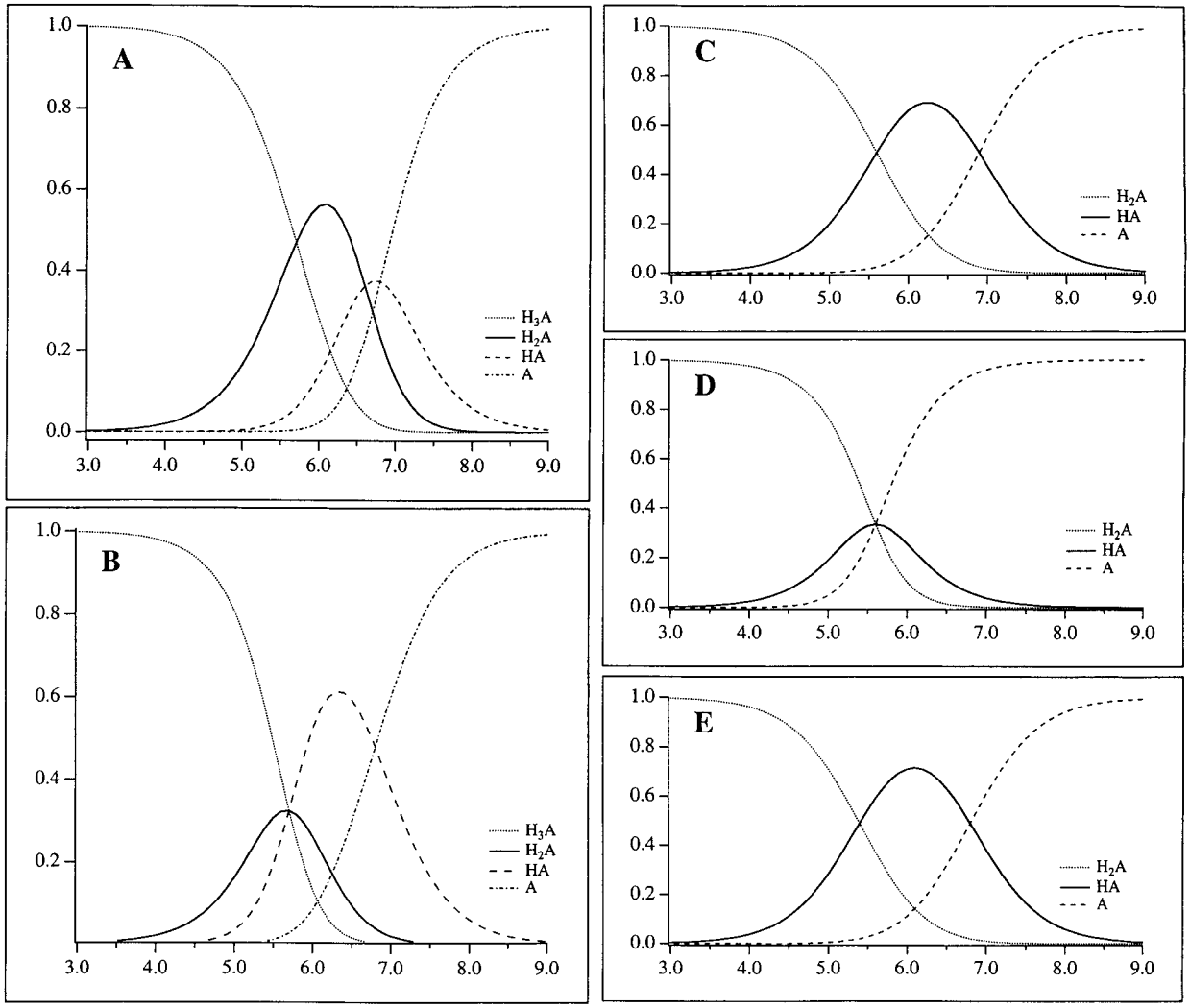

Figure 2. Calculated concentrations of the ionizing species in different states of protonation as a function of pH from the experimentally determined pK_a values: (A) MN, (B) JN, (C) JNI, (D) JNII, (E) JNIII. Curve assignments are given in each figure, where H_3A stands for polypeptide catalyst with three protonated His residues, etc.

first-order rate constant for the hydrolysis of mono-*p*-nitrophenyl fumarate is estimated to be 1×10^{-6} s^{-1} from the uncatalyzed reaction in aqueous buffer solution, although it is difficult to determine accurately due to the slow kinetics.

The second-order rate constant of the KO-42-catalyzed reaction is 0.31 M^{-1} s^{-1}, whereas that of the peptide MN is 0.027 M^{-1} s^{-1} and that of the peptide JN is 0.065 M^{-1} s^{-1}. The sum of the second-order rate constants of MN and JN is therefore less than the rate constant of KO-42. Consequently, there is cooperativity between helix I and helix II in KO-42 that is lost as the helices are "separated" and that accounts for a factor of 3.4 of the observed rate enhancement over that of the 4-MeIm-catalyzed reaction. To elucidate the cooperative role of the His residues in the neighboring helix, they were replaced by arginines. The reactivity of MN ($k_2 = 0.027$ M^{-1} s^{-1}) was increased by the introduction of Arg-30 and Arg-34 in helix II (MNRR, $k_2 = 0.080$ M^{-1} s^{-1}), and the reactivity of JNII ($k_2 = 0.054$ M^{-1} s^{-1}) was increased by the introduction of Arg-11 and Arg-15 in helix I (JNIIRR, $k_2 = 0.105$ M^{-1} s^{-1}). MNRR is 3 times as reactive as MN, and JNIIRR is twice as reactive as JNII, which contains His-30 and His-34. The interhelical cooperativity of KO-42 is therefore mainly due to electrostatic and hydrogen-bonded interactions since arginine side chains are poor nucleophiles and weak acids. The pK_a of an arginine side chain in a random coil peptide is 12.5.[9]

The peptide catalyst JN contains His-26, His-30, and His-34, and the reactivities of the sequences that contain the three pairwise combinations of His residues have been measured. The sum of the second-order rate constants for JNI (His-26 and His-30, $k_2 = 0.010$ M^{-1} s^{-1}) and JNII (His-30 and His-34, $k_2 = 0.054$ M^{-1} s^{-1}) is almost identical to that of JN ($k_2 = 0.065$ M^{-1} s^{-1}), the two pairwise sites His-30−His-34 and His-26−His-30 are therefore independent of each other, and the His-30−His-34 pair is the dominant site of helix II of KO-42. The reactivities of MNI (His-11 and His-15, $k_2 = 0.011$ M^{-1} s^{-1}) and MNII (His-15 and His-19, $k_2 = 0.008$ M^{-1} s^{-1}) do not add up to that of MN ($k_2 = 0.027$ M^{-1} s^{-1}), although the difference is small, and some cooperativity may therefore exist between the two sites in helix I of KO-42, perhaps because His-19 is not in a helical region[6] but in a loop.

The differences in reactivity between the peptides at pH 5.1 are due to the differences in nucleophilicities and to the different degrees of protonation and can be calculated from the Brønsted equation (eq 1) if the pK_a values of the catalytic histidines are

$$\log k_2 = A + \beta pK_a \quad (1)$$

$$\log k_2 = A - \alpha pK_a \quad (2)$$

(9) Tanford, C. *Adv. Protein Chem.* **1962**, *17*, 69.

known. At a pH below its pK_a a more acidic histidine is a more efficient catalyst than one with a higher pK_a, provided that $\beta < 1$. The nucleophilicity of a His residue decreases with pK_a as $10^{\beta pK_a}$, whereas the degree of protonation decreases roughly as 10^{pK_a}. At low pH the larger concentration of the unprotonated, and reactive, form of a nucleophile for a β of 0.8 outweighs its weaker nucleophilicity and is a more efficient catalyst by a factor of $10^{0.2\Delta pK_a}$.

The second-order rate constant of the JNIII-catalyzed reaction, 0.007 M^{-1} s^{-1}, is close to 0.0035 M^{-1} s^{-1}, which is that calculated for two noncooperative His side chains with pK_a values of 5.4 and 6.8 at pH 5.1, using a Brønsted coefficient β of 0.8,[10] the pK_a of 4-methylimidazole, 7.9, and its second-order rate constant 7.4×10^{-4} M^{-1} s^{-1}.[6] JNIII therefore does not show any cooperative behavior. The measured rate constant of the JNII-catalyzed reaction, 0.054 M^{-1} s^{-1}, is, however, much larger than those of two noncooperative His residues with pK_a values of 5.6, and it cannot be explained by differences in nucleophilicity and degrees of protonation alone. In order to probe the role of the flanking His residue, the kinetic solvent isotope effect was determined at pH 5.1, and the measured rate constant ratio $k(H_2O)/k(D_2O)$ for the JNII-catalyzed hydrolysis of mono-*p*-nitrophenyl fumarate was found to be 1.5. A kinetic solvent isotope effect that is larger than 1 shows that there is strong hydrogen bonding in the transition state, and the measured value therefore suggests general-acid catalysis in the pH range where JNII exists predominantly as $HisH^+-$His pairs.

The difference in second-order rate constants between the JNI- and JNII-catalyzed reactions can be analyzed using a model where the reactivity of the unprotonated His is calculated from the Brønsted equation for nucleophilic catalysis (eq 1) and the reactivity due to the flanking protonated His is calculated from the Brønsted equation for general-acid catalysis (eq 2). In JNII His-30 and His-34 have the same pK_a, 5.6, and in JNI the pK_a of His-26 is 6.9 and that of His-30 is 5.6. In JNII the reactivity is therefore the same regardless of which His is the nucleophile whereas JNI should be a more efficient catalyst if His-30 is the general acid since it has a lower pK_a. If there is a preference for the histidine with the higher number in the sequence to be the nucleophile, then His-30 with a pK_a of 5.6 would be the nucleophile in JNI and His-34 with a pK_a of 5.6 would be the nucleophile in JNII. The difference in reactivity is then mainly due to the difference in acidity of the proton donors, and a Brønsted coefficient α for general-acid catalysis of 0.65 would lead to a rate constant ratio of 5.4, eq 2, which is the experimental value, if the different degrees of protonation of the flanking His residues are taken into account. If the histidines with the lower sequence numbers were preferentially the nucleophiles, then the analogous argument would lead to a calculated rate constant ratio of 1.8, since in this case the only reactivity difference is that between the nucleophiles, whereas the pK_a values of the proton donors are the same.

Nucleophilic attack by His-34 and proton donation by His-30 in JNII and nucleophilic attack by His-30 and hydrogen bonding by His-26 in JNI are therefore strongly supported by the experimental results. The same analysis can be applied to show that His-15 is the nucleophile in MNI and His-19 is the nucleophile in MNII, although the difference in reactivity is smaller, and some uncertainty prevails in the understanding of the role of His-19.

Since the order of reactivities of JNII, MNI, and JNI after compensation for differences in nucleophilicities and degrees of protonation are in good agreement with general-acid catalysis by the flanking protonated $HisH^+$ residues, a lysine residue was introduced into MNI to reduce the pK_a values of His-11 and His-15 to test the conclusion that reactivity depends mainly on the pK_a of the reactive His residues. The pK_a of His-11 in MNI is 6.5, and that of His-15 is 6.1, but upon replacing Glu-14 by Lys-14 to form the sequence MNKI the pK_a values of both His-11 and His-15 were depressed to 5.6. The second-order rate constant for the MNI-catalyzed hydrolysis of mono-*p*-nitrophenyl fumarate is 0.011 M^{-1} s^{-1}, whereas that of MNKI is 0.041 M^{-1} s^{-1} in aqueous solution at pH 5.1. The increase in the second-order rate constant upon reducing the pK_a of both the nucleophile and the flanking protonated His is in good agreement with the conclusion that the $HisH^+-$His pair functions through cooperative nucleophilic and general-acid catalysis.

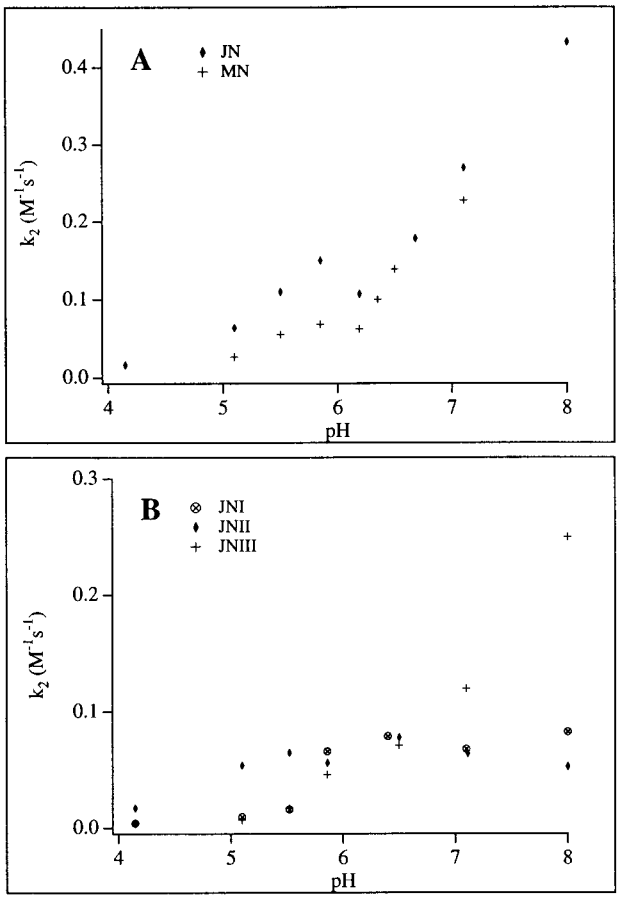

Figure 3. pH dependence of the second-order rate constants for the hydrolysis of mono-*p*-nitrophenyl fumarate in aqueous solution at 290 K: (A) JN- and MN-catalyzed reactions, (B) JNI-, JNII-, and JNIII-catalyzed reactions.

pH Dependence of the Histidine-Based Catalysts. The reactivity of the KO-42-catalyzed reactions is pH dependent,[6] and the pH profiles have been recorded for the most reactive catalysts derived from the sequence of KO-42, i.e., JN, MN, JNI, JNII, and JNIII (Figure 3). The pK_a values have been determined for all the histidine residues (Figure 1), and it is therefore possible to measure the reaction rates at a pH that is well above the pK_a of each histidine, where the only reactive species is the peptide with unprotonated His side chains. Unless there is a change in reaction mechanism at high pH, the second-order rate constants at low pH for reactions catalyzed by unprotonated histidines can be estimated from their dissociation constants. The reactivities at low pH of JN, MN, JNI, JNII, MNI, and MNII, which contain His residues in neighboring turns of helical segments, are too large to be compatible with catalysis

(10) Bruice, T. C.; Lapinski, R. *J. Am. Chem. Soc.* **1958**, *80*, 2265−2267.

by unprotonated peptides. The reactivities are therefore due to the mono- and diprotonated species, since the fully protonated ones have been shown to be unreactive. There is consequently cooperativity between protonated and unprotonated His residues in these peptide catalysts, which enhances substantially the reactivity of the $HisH^+$−His site, in good agreement with the conclusions drawn from the analysis of the kinetic measurements.

In reactions catalyzed by the peptide JN, the reactivity is high at pH 5.1, but due to the low and identical pK_a values of His-30 and His-34, the concentrations of mono- and diprotonated species are too similar to allow a discrimination between them from the pH dependence of the JN-catalyzed reaction alone. The pH dependence of the JNI-, JNII-, and JNIII-catalyzed reactions was therefore determined, and from the reactivities at pH 5.1 JNII was found to be the most efficient catalyst (Figure 3). At pH 5.1, the concentration of the monoprotonated form of JNII is more than 3 times as high as that of the unprotonated form and the concentration of the unprotonated catalyst is approximately 5% of that of the total amount of peptide. The limiting second-order rate constant of the JNII-catalyzed reaction at high pH is approximately 0.05 M^{-1} s^{-1}, and the calculated second-order rate constant due to the unprotonated catalyst at pH 5.1 is therefore on the order of 0.0025 M^{-1} s^{-1}, which is less than 5% of the observed rate constant for the JNII-catalyzed reaction of 0.054 M^{-1} s^{-1}. The reactive species in the JNII-catalyzed reactions at pH 5.1 is therefore predominantly the monoprotonated one. One unprotonated His side chain is necessary for catalysis, in agreement with the analysis of the second-order rate constants at pH 5.1, and the two-residue site of JNII in its monoprotonated form is capable of catalyzing the hydrolysis of mono-*p*-nitrophenyl fumarate with a second-order rate constant of 0.054 M^{-1} s^{-1}, which is more than 70 times larger than that of the 4-MeIm-catalyzed reaction. Supplementing this site with arginine residues in positions 11 and 15 doubles the rate constant, and optimization of the flanking residues in the neighboring helix may lead to even larger rate constants, substrate discrimination, and substrate binding.

The pH profiles of JN, JNI, and JNII are complex, but cooperativity is evident from the pH profile of JNII (Figure 3) since the absolute rate at pH 5.5, where the His residues of JNII are protonated to a large extent, is higher than that in the pH independent region at pH 8. The second-order rate constant for the JNI-catalyzed reaction titrates superficially with an apparent pK_a of approximately 5.7, although there are two His residues in the peptide with pK_a values of 5.6 and 6.9, a clear indication of differences in reactivity between partially protonated and fully unprotonated catalytic entities. In contrast, the titration of JNIII, which shows no cooperative kinetics, is compatible with the titration of two residues with pK_a values of 5.4 and 6.8, although the number of data points is not enough to show the complete transition. The pH profile of JN at low pH equals the sum of those of JNI and JNII, but at high pH the second-order rate constant of JN appears to be higher than the sum of those calculated for the individual histidines, suggesting a change in reaction mechanism. For example, the kinetic expression for "imidazole catalysis of imidazole catalysis" [11] contains higher order terms in imidazole that become significant at high pH, but the reaction mechanisms at high pH remain to be elucidated.

Conclusion. The results demonstrate that a two-residue site, consisting of an unprotonated His residue in position *i* and a $HisH^+$ residue in position $i - 4$, in a helical sequence functions through cooperative nucleophilic and general-acid catalysis. Its reactivity depends on the pK_a of the nucleophile as well as on the pK_a of the proton donor. Polypeptide catalysts capable of cooperative nucleophilic and general-acid catalysis are the most efficient, in comparison with the background reaction, the lower the pK_a of both residues in the $HisH^+$−His pair. Further transition state binding has been achieved by the introduction of arginine residues in the neighboring helix. This is the first example of a cooperative reactive site in a *de novo* designed four-helix bundle protein where the relationship between structure and reactivity has been demonstrated. Such sites are of general interest in the further development of designed protein catalysts toward substrate recognition and chiral discrimination.

Experimental Section

Peptide Synthesis, Purification, and Identification. The peptides were synthesized using a Biosearch 9600 or a PerSeptive Biosystems Pioneer automated peptide synthesizer using standard Fmoc chemistry protocols. The carboxy terminals were amidated upon cleavage from the resin by using a Fmoc-PAL-PEG-PS polymer (PerSeptive Biosystems). The amino terminals were capped with acetic acid anhydride. The peptides were cleaved from the polymer and deprotected with TFA (9 mL), anisole (200 μL), ethanedithiol (300 μL), and thioanisole (500 μL) for 2 h at room temperature. After diethyl ether precipitation and lyophilization, the peptides were purified by reversed phase HPLC on a semipreparative C-8 Kromasil, 7 μm column. The peptides were eluted isocratically using a solvent with 40−43% 2-propanol in 0.1% TFA, flow rates of 5 mL/min, and UV detection at 229 nm. The purity of each peptide was checked by reversed phase analytical HPLC. The identities of the peptides were determined by electrospray mass spectrometry (VG Analytical, ZabSpec). The obtained molecular weights were within 1 au of the calculated values, and no high molecular weight impurities could be detected. The purity of each peptide was estimated to be more than 95% from HPLC and ES-MS.

NMR and CD Spectroscopy. The ^{1}H-NMR spectra were recorded at 400 or 500 MHz using a Varian Unity 400 MHz or 500 MHz NMR spectrometer equipped with a matrix shim system from Resonance Research Inc. Peptide concentrations were about 0.4 mM, estimated from weighing, assuming a water content of 25%. The spectra were recorded in D_2O, and the pH (uncorrected) was adjusted by the addition of dilute DCl or NaOD. CD spectra were recorded on a Jasco J-720 spectropolarimeter, routinely calibrated with (+)-camphor-10-sulfonic acid. CD spectra were measured at room temperature in the wavelength interval 260−200 nm in a 0.1, 0.5, or 1 mm cuvette. The samples were prepared in buffer solution and diluted by pipetting to the desired concentrations, and the peptide concentrations of the stock solutions were determined by quantitative amino acid analysis. The pH dependence of the mean residue ellipticities of MN and JN was determined without buffer.

Kinetic Measurements. The kinetic experiments were carried out using a Varian Cary 1 or Cary 4 spectrophotometer equipped with a Varian temperature controller by following the absorbance at 320 nm (*p*-nitrophenol) or 405 nm (*p*-nitrophenolate) as a function of time. A stock solution of peptide in buffer was prepared, the pH was adjusted if necessary, and the solution was centrifuged before being diluted by pipetting to the desired concentrations. The buffers that were used were 100 mM sodium acetate in the pH range 4.2−5.5, 50 mM Bis-Tris from pH 5.9 to pH 7.1, and 50 mM Tris above pH 7.1, and the concentrations of the peptide stock solution were determined by quantitative amino acid analysis. In a typical kinetic experiment, 270 μL of peptide solution (0.2−0.5 mM) was thermally equilibrated in a 1 mm quarts cuvette, and 5 μL of substrate solution (7.4 mM) was added. The substrate mono-*p*-nitrophenyl fumarate was dissolved in 50:50 acetonitrile−buffer, and *p*-nitrophenyl acetate was dissolved in 100% acetonitrile. The reactions were followed for more than 2 half-lives, and the pseudo-first order rate constants were determined by fitting the experimental data to a single exponential function using Igor Pro software (Wavemetrics Inc.). The rate constants reported are the results

(11) Oakenfull, D. G.; Salvesen, K.; Jencks, W. P. *J. Am. Chem. Soc.* **1971**, *93*, 188−194.

from linear regression analysis of the experimentally measured pseudo-first-order rate constants as a function of three or more peptide concentrations. The errors in the reported second-order rate constants are due to errors in the linear regression analysis and the quantitative amino acid analysis. The error limits for the second-order rate constants are probably ±10%.

Acknowledgment. We are indebted to the Swedish Natural Science Research Council and Carl Tryggers Stiftelse for financial support.

JA9737580